

Testing coagulation potential of extracellular vesicles derived from aortic stenosis patients on human cardiac spheroids.

Name: Muhammad Nafiz Ikhwan Bin Nor Fuad

Supervisor: Avinash Khandagale (Ph.D. Dr. rer Hum. Biol.)

Date: VT 2023

**Course: Research Training in Medical Biochemistry and
Microbiology (3BL351)**

Department: Cardiology, Department of Medical Sciences.

Abstract

Cardiovascular diseases have always been the leading cause of global morbidity and mortality. Aortic stenosis, which is a kind of cardiovascular disease has a high prevalence in elderlies that are 75 years and older. Currently, the only available treatment would be valve replacement surgery. Recently, a few studies have risen regarding the potential of extracellular vesicles to reduce the effects of aortic stenosis, hence allowing patients to opt for a non-life-threatening treatment in comparison to a surgical one. The goal within this study is to determine the pro-coagulability of extracellular vesicles (EVs) that were endogenously derived from human blood (patients and healthy individuals) and their effect on the coagulation cascade. This study was performed on cardiac spheroids that were formed through seeding human aortic endothelial cells in an ultra-low attachment 96-well plate for 96 hours. Spheroids were challenged with tumour necrosis factor-alpha (TNF α) for 24 hours prior to EVs incubation for 48 and 72 hours. The effects of EVs on these spheroids were observed in terms of their ability to induce tissue factor activity. There was no significant difference in the tissue factor activity between spheroids incubated with patient derived EVs or healthy individual derive EVs irrespective of TNF α challenge. To conclude, the results of this study were not significant to stipulate that extracellular vesicles are procoagulant. Hence, further research regarding their ability to reduce or rescue the effects of cardiovascular diseases needs to be performed.

Keywords

Extracellular vesicles, human aortic endothelial cells, tissue factor, TNF α , coagulation pathway, cardiac spheroids

Introduction

Cardiovascular diseases (CVDs) have always been one of the top contributors to human mortality, especially in these recent years (Roth, et al., 2020). Within CVDs, valvular heart diseases (VHDs) are less known in comparison to coronary artery diseases. Aortic stenosis (AS) which is a VHD poses a huge risk towards the population, specifically to the elderly who is 75 years and older (Carità, et al., 2016). The aetiology of AS within this age group is poorly understood. That said, AS has been described to involve both complex inflammatory and fibroproliferative processes that to some extent had similarities to atherosclerosis. Nonetheless, there are no viable long-term treatments apart from surgical valve replacement. Hence, new studies are being done on novel pharmacotherapies (Goody, et al., 2020; Boskovski and Gleason, 2021; Natorska and Undas, 2015).

Extracellular vesicles (EVs) are described as membranous vesicles that are derived from cells. It is said that EVs play a crucial role in biological processes, specifically in the delivery of biological metabolites to recipient cells (Akbar, et al., 2019). There are two types of EVs namely exosomes and microvesicles. Exosomes are formed through inward budding of the cell membrane which results in an early endosome. These early endosomes undergo maturation to form the multivesicular bodies (MVBs), which is followed by the expulsion of MVBs' contents as exosomes through the process of exocytosis. Microvesicles are formed from the outward budding of the cell membrane. The cargoes that are being carried by these EVs can be both cell-specific and ubiquitous (Abels and Breakefield, 2016). This also indicates a slight difference in the proteome of different kinds of EVs. In terms of the cardiovascular system, EVs play a role in regulating the cardiomyocytes' survivability and also assist in heart tissue remodelling (Khandagale, et al., 2022). Recent studies have shown that EVs can be utilised further to tap their therapeutic potential for CVDs (Khandagale, et al., 2022; Fu, et al., 2020).

Spheroids are described as a group of cells that aggregates together to form a 3-dimensional structure. When first discovered, spheroids were usually utilized for cancer research. Spheroids have the potential to be used in all types of research.

This is due to the nature of these spheroids, specifically where they can imitate the function and structures of cellular tissues without a human body (Ryu, et al., 2019; Cesarz and Tamama, 2016). This results in a better simulation of cell to extracellular matrix interactions. Because of this unprecedented discovery, the implementation of spheroid transplantation as a means of treatment for degenerative diseases is slowly coming to real life (Cesarz and Tamama, 2016; Kawaguchi, et al., 2021). In terms of the cardiovascular system, the usage of spheroids is much preferred over 2-D cell cultures or animal models. The reason is that they can mimic the structure and function of cardiac cells (Polonchuk, et al., 2017). As spheroids are derived from patients' or healthy individuals' cells, it is easier to interpret the findings from cardiovascular research and implement them in a clinical trial. Finally yet importantly, spheroids can accurately replicate the early development of cardiomyocytes, especially the spatial organization (Polonchuk, et al., 2017; Kahn-Krell, et al., 2022).

The coagulation pathway is described as a process that prevents further bleeding that occurs from a tissue injury. The main 4 steps within this pathway are blood vessel constriction, platelet activation, coagulation cascade activation and fibrin plug formation. Within the coagulation pathway, there are 3 different pathways namely, the extrinsic, intrinsic and common pathway that is interdependent of one another (Palta, et al., 2014; Smith, et al., 2016). All 3 of these pathways are calcium-dependent and involve different types of coagulation factors. Different kinds of diseases may arise if any of these coagulation factors experience a temporary or permanent reduction.

The intrinsic pathway is triggered by the presence of endothelial collagen within the bloodstream due to an endothelial injury. This activates Factor XII which provides positive feedback downstream the pathway resulting in the activation of Factor VIII to form the platelet plug and activates Factor X. In a clinical diagnostic setting, the intrinsic pathway can be measured as partial thromboplastin time. The extrinsic pathway is triggered by endothelial tissue damage which releases Tissue Factor (TF) into the bloodstream and is activated. This pathway also involves Factor VII which is found circulating the body and requires vitamin K to be activated. Both activated TF and Factor VII will form a complex with activated Factor X in the common pathway.

In a clinical diagnostic setting, the extrinsic pathway can be measured as prothrombin time. The common pathway activates due to the activation of Factor X from either the intrinsic or extrinsic pathways. Activated Factor X will provide positive feedback downstream within this pathway, where Factor V, II, I and XIII get activated consecutively. By the end of this pathway, the fibrin plug is formed which marks the end of the coagulation pathway (Palta, et al., 2014; Smith, et al., 2016; Adams and Bird, 2009).

Aim

The purpose of this project is to observe and analyse the effects of extracellular vesicles on human aortic endothelial cells from patients that suffer from aortic valve stenosis, specifically in determining whether extracellular vesicles are procoagulant.

Materials and Methods

Cell Culturing Procedure

Human aortic endothelial cells (hAoECs) were purchased from PromoCell. hAoECs were cultured in phenol red-free endothelial cell basal medium supplemented with FCS-25 (final conc. 0.05 mL/mL), ECGS/H (final conc. 0.004 mL/mL), hEGF-5 (final conc. 10ng/mL), HC-500 (final conc. µg/mL) growth factors (purchased from Promocell) and penicillin (final conc. 50000 units/mL) and streptomycin (final conc. 50000 µg/mL) mixture (purchased from Invitrogen). The hAoECs were grown in a T25 cell culture flask containing 5 – 8 mL of medium within an atmosphere of 5% CO₂ incubator at 37°C. Trypsin-EDTA and trypsin neutralising solution were purchased from PromoCell. Trypsin-EDTA were used to passage confluent cells by releasing the cells from the culture flasks.

Once the hAoECs were confluent enough, the cell culture media was removed. Cells were washed with 2 mL of HEPES buffer (HBSS; 50 mM HEPES, pH 7, 145 mM NaCl, 5 mM KCl, 1,5 mM phosphate, 5,5 mM glucose). Then, Trypsin-EDTA (between 1.5 mL to 3 mL; according to flask size) was added followed by checking the flask under a microscope to detect cell detachment. When all cells had detached,

an equivalent volume of trypsin neutralising solution was added into the flask and the whole solution was transferred into a 15 mL Falcon tube. Followed by 6 mL of HBSS and centrifugation at 1400rpm for 5 minutes. The supernatant was removed and 3 mL of medium was added to resuspend the pellet. Upon resuspension, a cell count reading was performed by using the BioRad T20 Cell Counter following the manufacturer's instructions. According to the number of cells presents within the solution, different sizes of cell culture flask are utilized for cell splitting to form new passages.

Some of the hAoECs were cryofrozen for future uses. hAoECs (1×10^6) were cryopreserved in 1 ml of cryopreservation medium (CTS TM Synth-a Freeze TM, Gibco) in cryovials and stored at -80°C overnight prior to storage in liquid nitrogen.

Extracellular Vesicles Preparation

Blood samples retrieved in a citrated tubes were centrifuged for 15 mins at 2500g. The supernatant designated as platelet poor plasma (PPP), was extracted and placed into another tube. The PPP was then centrifuged for another 15 mins at 2500g and the supernatant, now called platelet free plasma (PFP) was extracted and placed into an ultracentrifuge tube. The PFP was ultracentrifuged at 20000g for 1 hour at $13 - 20^{\circ}\text{C}$. The supernatant was removed, and the pellet (EVs) were resuspended in 100 μL of HBSS buffer. The EVs were then stored in a -80°C freezer prior to use.

Spheroids Generation and incubation with EVs

Passage 5 hAoECs were chosen to generate the spheroids. The hAoECs at different initiating cell densities were seeded in an ultra-low attachment 96-well plate, where they were seeded in the media (100 μL) for a total of 96 hours in a 5% CO_2 incubator at 37°C . The spheroids were observed every 24 hours to ensure their viability and progression. At the 48-hours post-incubation mark, EVs from different patient groups were introduced at concentration of 50 $\mu\text{g}/\text{mL}$. Four groups of samples were included in the experiments: a control group (K) without any addition, a group with EVs from healthy individuals (Hc), one with patients' EVs isolated after the patient's first hospital visit (V0) and a fourth with EVs isolated from the patients

after their second hospital visit (V1). After 72 hours of spheroid generation, TNF α (25 ng/mL) was introduced. The spheroids were then left to incubate for another 24 hours, 48 hours and 72 hours with or without EVs.

Spheroids' Supernatants and Lysates

Media from spheroids incubated with EVs were collected and subsequently utilized as spheroid supernatant samples. 50 μ L of RIPA lysis buffer (50 mM Tris/HCl, pH 7.4, 150 mM NaCl, 1 % Nonidet P-40, 0.5 % sodium deoxycholate, 0.1 % sodium dodecyl sulfate) was added to each well to lyse the spheroids. Both supernatant and lysates were stored at -20°C before further use.

To ensure that the spheroids samples were not contaminated by mycoplasma, Invivogen MycoStrip test were performed. Supernatants first collected from spheroid samples were prepared in accordance with the Invivogen MycoStrip manual. The principle behind this Mycoplasma Detection Kit is that 16s rRNA gene is being targeted and amplified by the Invivogen reaction mix. The reaction mix will then bind to the 16s rRNA gene to form a complex that will change the immunochromatographic strip from colourless to red. If distinct red band appear on both the control (C) and test (T) sections of the kit, this indicates that there have been contaminations. This is because mycoplasma is a bacterium that produces this gene at high concentrations, eventually leading to ribosome production which is an important molecule of the protein synthesis process. Once prepared, 100 μ L of the processed lysate was added to the assay cassette. The results of the detection kit were then observed and interpreted after 2 – 5 minutes.

Protein Determination

Bovine serum albumin (BSA, Sigma-Aldrich) was prepared as 200 mg/mL stock in HBSS (50 mM HEPES, pH 7, 145 mM NaCl, 5 mM KCl, 1,5 mM phosphate, 5,5 mM glucose). and used as two-fold dilution series. A BIORAD DC Protein Assay was performed with 10 μ L of BSA sample in 96-well plate according to the manufacturers protocol and read by spectrophotometry at 750 nm.

Tissue Factor Activity Assay

Dade Innovin reagent was prepared to be used as a standard for the tissue factor (TF) activity assay. The principle behind this assay is that, both TF and Factor VII complex will produce activated Factor X, which will then bind to a chromogenic substrate which can be measured spectrophotometrically at 405nm.

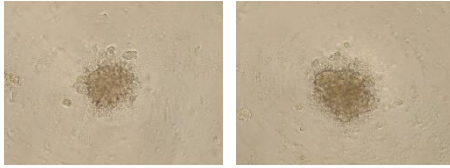
From the stock Innovin reagent (10 ng/mL), 10-fold serial dilutions were prepared in a 96-well plate. 20 μ L of CaCl_2 solution (final conc. 50mM) was added into each well of a 96-well plate which was followed by the addition of 20 μ L of the standard and/or samples that will be examined into each well. Next, a master mix which consists of 0.076 μ L of Factor VII (final conc. 50 nM) and 0.284 μ L of Factor X (final conc. 100 nM) mixed in a 9.64 μ L of HBSS (50 mM HEPES, pH 7, 145 mM NaCl, 5 mM KCl, 1,5 mM phosphate, 5,5 mM glucose) was made. 10 μ L of the master mix was added to each well. The 96-well plate was then placed in a 37°C incubator. After 2 hours, 12.5 μ L of substrate (final conc. 0.67 mM) was added into each well, followed by another 30 minutes incubation in a 37°C incubator. At the end of the incubation period, the 96-well plate was read in a spectrophotometer at 405nm, where the data were collected and calculated.

Results

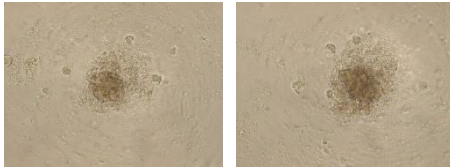
Spheroids Generation

To determine which cell density would be best to examine the TF activity of the spheroids, duplicates of spheroids at 4 different cell densities were produced and observed at 4 different time-points (Fig. 1). At all 4 time-points, all 4 cell densities had some similarities and differences. For all of these cell-density groups, EVs from patients, healthy individuals and controls were introduced after the 48 hours timepoint.

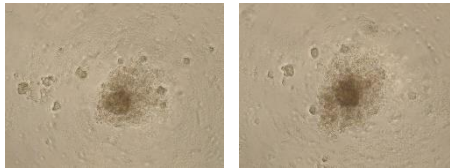
A 2000-cells spheroids



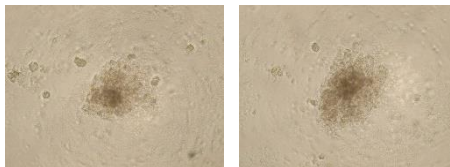
24
hours



48
hours

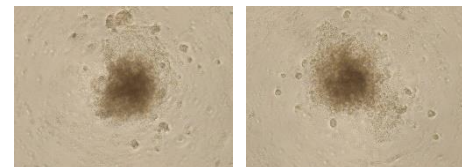
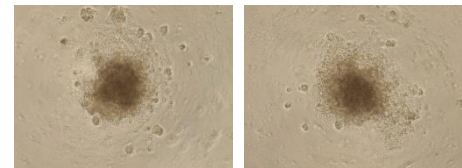
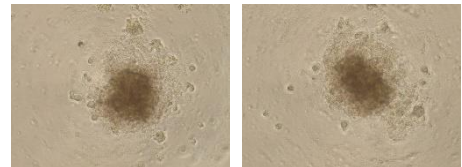
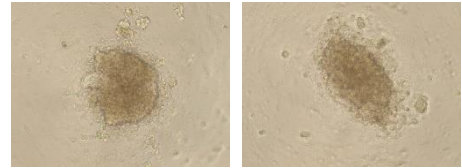


72
hours

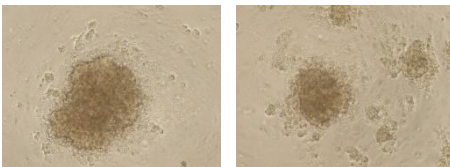


96
hours

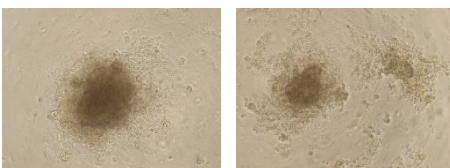
B 5000-cells spheroids



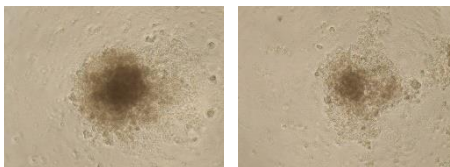
C 10000-cells spheroids



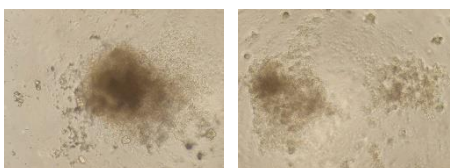
24
hours



48
hours



72
hours



96
hours

D 20000-cells spheroids

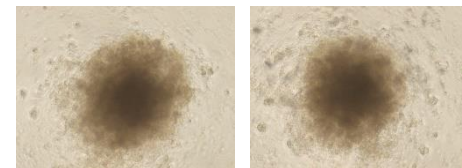
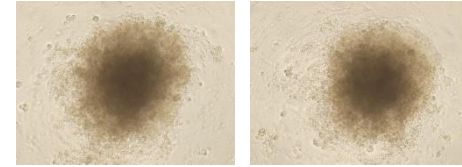
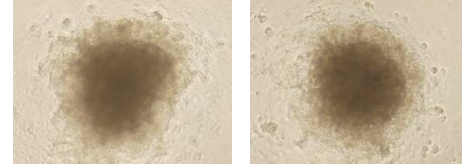
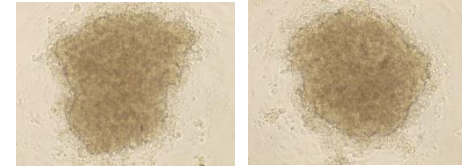


Fig. 1. Spheroids formation at different time-points (2000, 5000, 10000, and 20000-cells). hAoECs were treated with EVs 48 hours post-incubation, followed by TNF α introduction 24 hours post-EVs. These hAoECs were observed under a microscope at 24-hours, 48-hours, 72-hours, and 96-hours post-incubations time points. (A) 2000-cells. (B) 5000-cells. (C) 10000-cells (D) 20000-cells.

Both 2000 and 5000 cell density spheroids were able to form the core of a spheroid at the 24-hour time-point. However, the cells did not adhere together to form a larger and rounder spheroid after prolonged incubation. This was observed in both duplicates (Fig. 1A and 1B). By the end of the 96-hours time-point, spheroids were not formed, and the cells were just scattered.

The 10000 cell samples (Fig. 1C), both duplicates managed to form the spheroid core at the 24-hour time-point. However, as the incubation time went on, only the first duplicate managed to form a non-spherical spheroid while the other failed. The surrounding cells of the second duplicate did not integrate into the centrally formed spheroid but instead formed islands (Fig. 1C). These cell-density spheroids were utilized for the protein concentration determination assay against the BSA standard.

The 20000 cell starting condition (Fig. 1D), led in both duplicates to the formation of a spheroid core 24 hours of growth. This development was further observed at the 48 hours and 72-hours time-point. In comparison to the other cell-density groups, the 20000 group formed a darker spheroid core due to a lot more necrotic cells were present within the core itself. By the end of the 96-hours time-point, both duplicates managed to form spheroids, just a proper non-spherical one (Fig. 1D). As 20000 cell density spheroids possessed a high amount of cells, they were utilized for the TF activity assay against the Innovin Standard.

Mycoplasma Detection

To detect the presence of mycoplasma's 16s rRNA gene within the spheroids' supernatant, a mycoplasma detection kit was utilized. The 16s rRNA gene is important for the mycoplasma as it produces the ribosomes which are involved in the translation process of protein synthesis. The control (C) region of the detection kit displays a distinct red band while the test (T) region of the detection kit displays no

band. This indicated that there were no 16s rRNA gene present within our spheroids' growth media, which meant that our samples most probably had not been contaminated by mycoplasma.

Tissue Factor Activity Assay

To determine whether the introduction of EVs from different patient groups, post-TNF α addition, would have an increased TF activity, a Tissue Factor activity assay was performed.

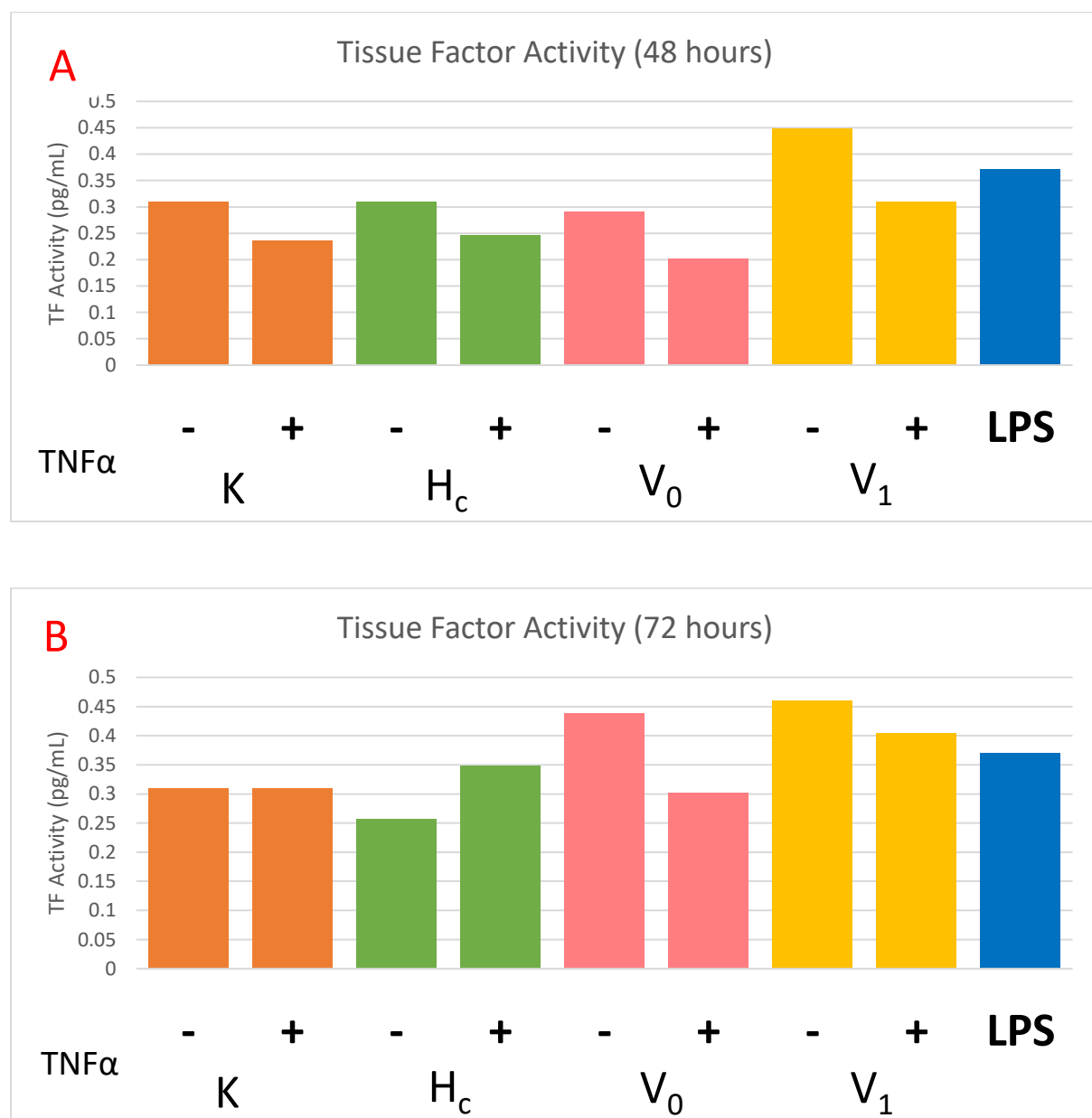


Fig. 2. Tissue Factor activity determination after stimulation of spheroids with EVs and TNF α at different time-points. hAoECs spheroids were treated with EVs of different patient groups after 48 hours of spheroid growth; K (control group, no EV added), H_c (EV from healthy individual), V₀ (AS EVs isolated from blood at patient's first visit), V₁ (AS EVs isolated from blood at patient's second visit) and LPS (lipopolysaccharide) which was added at the same time as EVs introduction. TNF α was added (+) or omitted (-) 24 hours thereafter and the spheroid growth followed another 48 (**A**) or 72 hours (**B**) before samples were prepared for analysis.

We observed that the 20000-cells density spheroid lysates of all groups within the 48 hours post TNF α -addition, had similar TF activity when compared to their own control samples (Fig. 2A). These values are an indication that there were low amounts of TF activity within all of these spheroids. Lipopolysaccharide (20 μ g/mL) derived from gram-negative bacteria's cell wall acted as positive control. It seems that the control sample of the V₁ group had higher values compared to the LPS positive control. This value informed us that the introduction of the EVs was somewhat procoagulant.

After 72 hours of TNF α incubation, similar results could be observed (Fig. 2B). Surprisingly, it was determined that there was an increase in TF activity for the experimental samples of the V₀ and V₁ group, from the 48-hour time point to the 72-hour time point. Not only did this happen to the experimental samples of V₀ and V₁ group, but it also happened to the control samples of the same group. That said, there was variability in the TF activity between the two-time-points of a group, for example, the control sample of the H_c group. Overall, all groups had similar amount of TF activity independent of their incubation period and conditions. Arguably, there are slight differences amongst each groups' samples, however, these differences were non-significant.

Discussion

A recent study determined that the size and structure of the spheroids are independent of the initial cell density seeded (Browning, et al., 2021). We performed this study to better understand and find the correlation between initial seeded cell density and the size of spheroids formed. As we generated our spheroids, we found that the spheroids' size and structure are somewhat dependent on the number of cells seeded to form these spheroids. As observed in Fig. 1, 20000 cells were able to form a spheroid, despite this being non-spherical. However, 2000 cells and 5000 cells were only able to form the core of a spheroid. A spheroid core is characterized by the necrotic cells that are in the middle of the spheroid. These cells are often seen to be darker compared to the other cells that surrounds them (Fig. 1). When comparing the 20000-cells spheroids and 10000-cells spheroids, a difference in size could also be seen where the 20000-spheroids had a larger diameter whilst the 10000-spheroids had a smaller one. We believed that a more thorough experiment should be done to determine if the correlation between the two variables is strong, if any.

We observe that the 2000 cells and 5000 cells did not adhere together but rather scattered around (Fig. 1). This could be due to the seeded cell number was too little for a successful spheroid generation. Moreover, one of the 10000-cells spheroids duplicates was able to form a spheroid while the other failed. It seems that the second duplicate was not able to integrate into the spheroid core but instead formed islands surrounding the spheroids. One reason could be that, the cells did not managed to detach from each other, which eventually leads to clumps formation (islands). As for the 20000 cells spheroids, both duplicates were able to form spheroids after 96 hours despite the outer layer of the spheroids were not fully formed. This may be due to the lack of proper cell solution mixing at start.

Once the standard has been established and spheroids generation was successful, the protein concentration of these spheroids could then be determined. The reason why we performed protein detection was to ensure that the spheroids are undergoing

homeostasis and they form the necessary proteins. We observed that all the 20000 cells spheroids possess a relatively similar protein concentration to each other.

A review by Nikfarjam and Farzaneh (2012) established that mycoplasma contamination is common in cell cultures. Hence, to ensure that the values of the control groups that were calculated within the TF activity assay were not influenced by the presence of any mycoplasma, a mycoplasma detection test was performed. The principle behind is that 16s rRNA gene binds to the Invivogen reaction mix which forms a complex that will change the immunochromatographic strip from colourless to red. These genes are present at high concentration especially, as it leads to the production of ribosome which is a part of the translation process of protein synthesis. Hence, we deduced that our samples were not contaminated, and the control group values were not altered.

In a recent study done by Nakatani, et al. (2022), they discovered that EVs derived from 3T3-L1 adipocytes were procoagulant. They had also mentioned that the procoagulant effects of these adipocyte-derived EVs were further enhanced upon stimulation by TNF α . However, we did not find EVs isolated from AS patients being procoagulant. These EVs showcased poor TF activity by themselves and failed to render procoagulant effects to spheroids generated by hAoECs. This could be due to the fact that our study was utilizing EVs that were derived from patients' blood plasma and tested on hAoECs spheroids, while Nakatani, et al. derived the EVs from mouse models and experimented on human plasma instead of spheroids.

TNF α priming is known to activate endothelial cells and may results in an increase in endothelial procoagulant potential. Therefore, we primed hAoEC generated spheroids (that has been incubated with different sets of EVs from either healthy or AS patients) with TNF α . We did not see increase TF activity post TNF α priming by hAoEC spheroids suggesting that TNF α does not induce endothelial procoagulant capacity both at 48 hours and 72 hours' time-points. In addition, we have utilized bacterial lipopolysaccharides (LPS) to induce endothelial spheroids' procoagulant ability to be served as a positive control. However, LPS treatment failed to instigate TF activity by spheroids. This may be due the concentrations utilised in these

experiments were too low. Calibrations with different concentration of these inducers at different time-points need to be checked for their effectiveness in terms of TF activity generation.

To test EVs' procoagulant potential we tested different sets of EVs from healthy individuals and AS patients on both TNF α primed and unprimed hAoECs spheroids. It is noted that overall TF activity was very small in all tested samples, however, EVs from AS patients showed slightly increased TF activity compared to EVs from Hc group irrespective of TNF α priming of spheroids. This is seen in the experimental sample of V₁ group (AS patient) at the 48-hour time point and the experimental samples of both V₀ and V₁ group (AS patient) at the 72-hour time point. These results, although not significant displays procoagulant trend of AS derived EVs which needs to be consolidated further with additional experiments and an increased number of patient samples.

In conclusion, procoagulant capacity of EVs derived from human blood from AS patients could not be determined on hAoECs spheroids irrespective of TNF α priming of these spheroids. However, it can not be concluded entirely that AS patient derived EVs are not procoagulant based on these limited number of experiments which also included technical inadequacies and inexperienced hands. Further research should be done to better understand the effects of EVs from patients suffering from cardiovascular diseases on complex cardiac environment and the alterations they caused within the pathway to rescue or deteriorate the conditions.

Acknowledgement

Fullest gratitude to Christina Christersson for allowing myself the opportunity to pursue a research training course in her research lab and providing sufficient resources. Special thanks to Avinash Khandagale for supporting and mentoring throughout the whole process of this study. Special thanks to Ebba-Louise Skogseid for sharing her research findings and knowledge in cardiology.

References List

Abels, E. R., and Breakefield, X. O. (2016). Introduction to extracellular vesicles: Biogenesis, RNA cargo selection, content, release, and uptake. *Cell. Mol. Neurobiol.* 36(3), 301–312.

Adams, R. L. C., and Bird, R. J. (2009). Review article: Coagulation Cascade and therapeutics update: Relevance to nephrology. part 1: Overview of coagulation, Thrombophilias and history of anticoagulants. *Nephrol.* 14(5), 462–470.

Akbar, N., Azzimato, V., Choudhury, R. P., and Aouadi, M. (2019). Extracellular vesicles in metabolic disease. *Diabetologia.* 62, 2179-2187.

Boskovski, M. T., and Gleason, T. G. (2021). Current therapeutic options in aortic stenosis. *Circ. Res.* 128(9), 1398–1417.

Browning, A. P., Sharp, J. A., Murphy, R. J., Gunasingh, G., Lawson, B., Burrage, K., Haass, N. K., and Simpson, M. (2021). Quantitative analysis of tumour spheroid structure. *ELife.* 10.

Carità, P., Coppola, G., Novo, G., Caccamo, G., Guglielmo, M., Balasus, F., Novo, S., Castrovinci, S., Moscarelli, M., Fattouch, K., and Corrado, E. (2016). Aortic stenosis: insights on pathogenesis and clinical implications. *J. Geriatr. Cardiol.* 13(6), 489.

Cesarz, Z., and Tamama, K. (2016). Spheroid culture of mesenchymal stem cells. *Stem Cells Int.* 2016, 1–11.

Fu, S., Zhang, Y., Li, Y., Luo, L., Zhao, Y., and Yao, Y. (2020). Extracellular vesicles in cardiovascular diseases. *Cell Death Discov.* 6(1), 68.

Goody, P. R., Hosen, M. R., Christmann, D., Niepmann, S. T., Zietzer, A., Adam, M., Bönner, F., Zimmer, S., Nickenig, G., and Jansen, F. (2020). Aortic valve stenosis. *Arterioscler. Thromb. Vasc. Biol.* 40(4), 885–900.

Kahn-Krell, A., Pretorius, D., Guragain, B., Lou, X., Wei, Y., Zhang, J., Qiao, A., Nakada, Y., Kamp, T. J., Ye, L., and Zhang, J. (2022). A three-dimensional culture system for generating cardiac spheroids composed of cardiomyocytes, endothelial cells, smooth-muscle cells, and cardiac fibroblasts derived from human induced-pluripotent stem cells. *Front. Bioeng. Biotechnol.* 10.

Kawaguchi, S., Soma, Y., Nakajima, K., Kanazawa, H., Tohyama, S., Tabei, R., Hirano, A., Handa, N., Yamada, Y., Okuda, S., Hishikawa, S., Teratani, T., Kunita, S., Kishino, Y., Okada, M., Tanosaki, S., Someya, S., Morita, Y., Tani, H., Kawai, Y., Yamazaki, M., Ito, A., Shibata, R., Murohara, T., Tabata, Y., Kobayashi, E., Shimizu, H., Fukuda, K., and Fujita, J. (2021). Intramyocardial transplantation of human IPS cell-derived cardiac spheroids improves cardiac function in heart failure animals. *JACC: Basic Transl. Sci.* 6(3), 239–254.

Khandagale, A., Lindahl, B., Lind, S. B., Shevchenko, G., Siegbahn, A., and Christersson, C. (2022). Plasma-derived extracellular vesicles from myocardial infarction patients inhibits tumor necrosis factor-alpha induced cardiac cell death. *Curr. Res. Transl. Med.* 70(2), 103323.

Lowry, O. H., Rosebrough, N. J., Farr, A. L., and Randall, R. J. (1951). Protein measurement with the Folin phenol reagent. *J. Biol. Chem.* 193(1), 265–275.

Nakatani, E., Naito, Y., Ishibashi, K., Ohkura, N., and Atsumi, G.-ichi. (2022). Extracellular vesicles derived from 3T3-L1 adipocytes enhance procoagulant activity. *Biol. Pharm. Bull.* 45(2), 178–183.

Natorska, J., and Undas, A. (2015). Blood coagulation and fibrinolysis in aortic valve stenosis: Links with inflammation and calcification. *Thromb. Haemost.* 114(08), 217–227.

Nikfarjam, L., and Farzaneh, P. (2012). Prevention and detection of Mycoplasma contamination in cell culture. *Cell Journal (Yakhteh)*, 13(4), 203.

Palta, S., Saroa, R., and Palta, A. (2014). Overview of the coagulation system. *Indian J. Anaesth.* 58(5), 515.

Polonchuk, L., Chabria, M., Badi, L., Hoflack, J.-C., Figtree, G., Davies, M. J., and Gentile, C. (2017). Cardiac spheroids as promising in vitro models to study the human heart microenvironment. *Sci. Rep.* 7(1).

Roth, G. A., Mensah, G. A., Johnson, C. O., Addolorato, G., Ammirati, E., Baddour, L. M., Barengo, N. C., Beaton, A. Z. Benjamin, E. J., Benzinger, C. P., Bonny, A., Brauer, M., Brodmann, M., Cahill, T. J. Carapetis, J., Catapano, A. L., Chugh, S. S., Cooper, L. T., Coresh, J., Criqui, M., DeCleene, N., Eagle, K. A., Emmons-Bell, S., Feigin, V. L., Fernández-Solà, J., Fowkes, G., Gakidou, E., Grundy, S. M., He, F. J., Howard, G., Hu, F., Inker, L., Karthikeyan, G., Kassebaum, N., Koroshetz, W., Lavie, C., Lloyd-Jones, D., Lu, H. S., Mirijello, A., Temesgen, A. M., Mokdad, A., Moran, A. E., Muntner, P., Narula, J., Neal, B., Ntsekhe, M., Moraes de Oliveira, G., Otto, C., Owolabi, M., Pratt, M., Rajagopalan, S., Reitsma, M., Ribeiro, A. L. P., Rigotti, N., Rodgers, A., Sable, C., Shakil, S., Sliwa-Hahnle, K., Stark, B., Sundström, J., Timpel, P., Tleyjeh, I. M., Valgimigli, M., Vos, T., Whelton, P. K., Yacoub, M., Zuhlke, L., Murray, C., Fuster, V., and GBD-NHLBI-JACC Global Burden of Cardiovascular Diseases Writing Group. (2020). Global burden of cardiovascular diseases and risk factors, 1990–2019: update from the GBD 2019 study. *J. Am. Coll. Cardiol.* 76(25), 2982-3021.

Ryu, N.-E., Lee, S.-H., and Park, H. (2019). Spheroid culture system methods and applications for mesenchymal stem cells. *Cells.* 8(12), 1620.

Smith, S. A., Travers, R. J., and Morrissey, J. H. (2015). How it all starts: Initiation of the clotting cascade. *Crit. Rev. Biochem. Mol Biol.* 50(4), 326–336.